

An Ab Initio Study of the Potential Energy Surface of the Reaction $\text{CHCl}^{2+} + \text{H}_2$ and Comparison with Experimental Data

Jana Roithová, Jan Hrušák, and Zdenek Herman*

V. Čermák Laboratory, J. Heyrovský Institute of Physical Chemistry,
Academy of Sciences of the Czech Republic, Dolejškova 3, CZ-182 23 Prague 8, Czech Republic

Received: April 24, 2003; In Final Form: June 19, 2003

Reaction pathways that lead to products of the reactions in the $[\text{CHCl}]^{2+} + \text{D}_2$ system (CHCl^+ , CCl^+ , CHDCl^+ , HD_2^+ , D_2^+ , as observed experimentally) were studied using the CCSD(T)/cc-pVTZ method. Energies of located stationary points on the potential energy hypersurface were refined by the G2 method. Both isomers of the reactant dication CHCl^{2+} — HCCl^{2+} (with H atoms bonded to C atoms) and CClH^{2+} (with H atoms bonded to Cl atoms)—were taken into consideration. The calculated reaction pathways were of importance in the interpretation of experimental beam-scattering data. The heats of formation of the reactant dications HCCl^{2+} and CClH^{2+} and of all relevant products ions (CCl^+ , HCCl^+ , CClH^+ , H_2CCl^+ , HCClH^+) were calculated.

1. Introduction

The chemical reactivity of small molecular dications and their unusual features recently have been attracting an increasing amount of attention from chemists. The unusual features of the chemical reactivity of dications include high energy content of the reactants, high exoergicity of chemical reactions, the formation of electronically excited products, frequent further dissociation of primary reaction products, and the formation of a pair of singly charged products and Coulomb repulsion between them, leading to high translational energy of products, the formation of fast “naked” protons in reactions with hydrogen, impulsive proton-transfer reactions of hydrogen-containing molecular dications, etc. Most molecular dications are metastable, with respect to decomposition to two thermodynamically more stable singly charged ions. The ionization energies of molecular cations to form dications are usually 15–30 eV, and the dications easily react in charge transfer and dissociative charge-transfer processes.

Bond-forming reactions of molecular dications¹ have been observed in an increasing number of systems. They occur typically in competition with charge-transfer processes that often dominate among the reaction products. Dissociative processes, both for charge transfer and chemical reactions, are rather frequent. More-detailed studies have been conducted on systems such as $\text{CF}_2^{2+} + \text{D}_2$,^{2,3} HD ,^{4,5} $\text{CO}_2^{2+} + \text{D}_2$,⁶ HD ,⁷ and $\text{CF}_3^{2+} + \text{HD}$.^{7,8} The CHCl^{2+} dication represents a rather different system than CF_2^{2+} , CF_3^{2+} , or CO_2^{2+} . The presence of a H atom suggests a strong acidic nature,⁹ which should affect its reactivity.

A motivation for this study comes from the investigation of the dynamics of chemical reactions and charge-transfer processes in collisions of the molecular dication CHCl^{2+} with deuterium¹⁰ and noble gases¹¹ in crossed-beam scattering experiments. In the reaction with D_2 , three main products were identified, namely CHCl^+ , CCl^+ , and CHDCl^+ .¹⁰ Contour diagrams of the ion products, relative differential cross sections, and relative translational-energy distribution of the products were obtained from the scattering experiments, and conclusions on the dynam-

ics of the processes could be made. The product ion CHCl^+ was shown to originate from a nondissociative charge-transfer process of the ground and excited states of two isomers of the reactant dication, namely HCCl^{2+} and CClH^{2+} (i.e., with the H atom being bonded either to the C atom or to the Cl atom). An experimental¹¹ and theoretical¹² study of charge transfer with noble gases helped to identify the respective state-to-state processes. The chemical reaction products were $\text{CHDCl}^+ + \text{D}^+$, formed in processes that involved the formation of reaction intermediates of two different mean lifetimes, presumably in reactions of both molecular dication isomers. Finally, CCl^+ was shown to be formed mainly in an impulsive chemical reaction of proton transfer (the other product was HD_2^+) from the reactant HCCl^{2+} in the ground state; a portion of this product was formed in further dissociation of the chemical reaction product CHDCl^+ . The proton-transfer reaction was confirmed by measuring integral cross sections of the reactions with D_2 .^{11,13} and identification of both reaction products of the proton-transfer process. Similar results were obtained for the reaction of CHCl^{2+} with argon (which resulted in the formation of $\text{CCl}^+ + \text{ArH}^+$).¹³

Considerable attention has been given to the dication CHCl^{2+} . An experimental study¹⁴ identified the dication CHCl^{2+} as a long-lived fragment of $\text{CH}_3\text{Cl}^{2+}$. In a theoretical study,¹⁵ dissociation channels of the dication $\text{CH}_3\text{Cl}^{2+}$ were studied and partial information on the potential energy surface was obtained. A complete active space-self-consistent field calculation, together with the TZP basis set (CASSCF/TZP), was used in this study. However, the authors referred to the $\text{H}-\text{C}-\text{Cl}^{2+}$ isomer only. This work, as well as several others,^{10,16,17} pointed out the important rearrangement of the chloromethane dication, which leads to the dication of its ylide form, $\text{CH}_2\text{ClH}^{2+}$.

The aim of the present study is to calculate the potential energy hypersurface (PES) of the $\text{CHCl}^{2+} + \text{H}_2$ system at a uniform and reliable level of theory and to provide sufficiently accurate data for the interpretation of previous experimental results of crossed-beam studies of charge transfer and chemical reactions in this system.

2. Computational Method

The calculations were performed using the coupled cluster method CCSD(T),^{18–21} in conjunction with Dunning’s correla-

* Author to whom correspondence should be addressed. E-mail: zdenek.herman@jh-inst.cas.cz.

tion consistent triple- ζ basis set (cc-pVTZ),^{22–24} as implemented in the Gaussian 98 method.²⁵ For all the optimized structures, frequency analysis at the same level of theory was used to assign them as real minima and transition structures on the PES. Energies of all the stationary points were refined by the G2 method.²⁶ The G2 energies were calculated for the CCSD(T) optimized structures and include the CCSD(T) zero-point vibrational energy. All the structures were pre-optimized at the density functional theory level, using the same basis set (B3LYP/cc-pVTZ). The basis set superposition error was calculated for the loosely bound complexes (see Section 3.3.1 presented later in this paper) and was observed to be practically negligible (<0.01 eV).

3. Results and Discussion

For the reactant CHCl^{2+} , two possible stable isomers— HCCl^{2+} and CClH^{2+} , with H atoms bonded either to C or to Cl atom, respectively—were taken into consideration. The basic aim of this study was to construct the singlet PES that corresponds to the ground states of both isomers. In addition, several structures were optimized in the triplet electronic states to complete the overall picture (these structures are denoted with an asterisk (*)). All optimized structures, i.e., the minima and the transition states, are shown in Figure 1. The CCSD(T) total energies (ϵ_0), the zero-point energy (ZPE) corrections (ϵ_{ZPE}), and G2 energies (E_0) are given (in hartrees) in Table 1. Table 2 lists the relative energies ($\Delta\epsilon_0$)_{rel.}, ($\Delta(\epsilon_0 + \epsilon_{\text{ZPE}})$)_{rel.}, and (ΔE_0)_{rel.} of the individual points on the reaction hypersurface. The relative values are related to the energy of $\text{HCCl}^{2+} + \text{H}_2$ and have been recalculated in terms of electron volts. Minima on the PES (all frequencies are real) are denoted as **Mx** (x indicates a number), whereas the transition structures (those which possess one imaginary frequency) are denoted as **TSx** (x is a number).

The dication HCCl^{2+} (**M1**) has a linear structure with a very short C–Cl bond (1.48 Å), because it is an efficient overlap of the C and Cl bonding orbitals, which leads formally to a triple bond between these both partners. The first excited triplet state (**M1***) lies 4.23 eV above it and has a bent geometry. The other isomer, C–Cl–H²⁺ (**M3**), is higher in energy than H–C–Cl²⁺(**M1**), by 3.02 eV. In the isomer M3, the C–Cl bond is a single bond and, thus, is correspondingly longer (1.74 Å). The two lone pairs of electrons located on Cl atom lead to a bent geometry, with a bonding angle of 94.4°. The isomerization of these two dications ($\text{HCCl}^{2+} \leftrightarrow \text{CClH}^{2+}$) proceeds via the transition state **TS1**. The barrier height calculated for this isomerization ($\text{HCCl}^{2+} \rightarrow \text{CClH}^{2+}$) is 3.83 eV. For the reverse process ($\text{CClH}^{2+} \rightarrow \text{HCCl}^{2+}$), the calculation gives a barrier height of 0.81 eV. The first triplet excited state of the dication CClH^{2+} (**M3***) lies 2.08 eV above the ground state. The detailed computational study of the ground state and the low-lying excited states of both dication isomers, HCCl^{2+} and CClH^{2+} , has been published separately.¹² The method applied was the averaged quadratic coupled cluster method (AQCC), using complete active reference space and a moderate atomic natural orbital basis set. This method is regarded as quite accurate for calculations of excited states and can be viewed as a multi-reference approach to the coupled cluster method, as presented here. The results for the single reference AQCC converge to the CCSD, as demonstrated by small differences of ~ 0.02 eV between the energies calculated with the use of the CCSD(T) and AQCC methods. The excitation energies from the singlet ground state to the first excited triplet state, obtained with the AQCC–CASSCF method, were 4.13 eV for HCCl^{2+} (CCSD(T) calculations gave a value of 4.12 eV) and 1.94 eV for CClH^{2+}

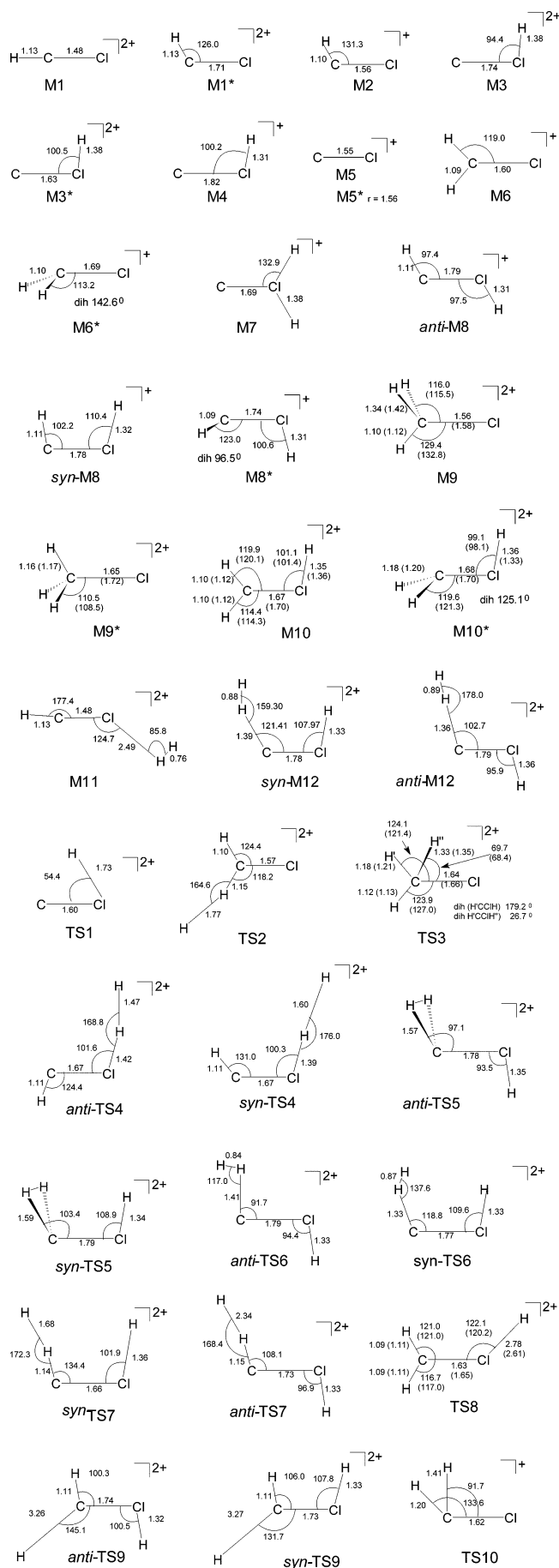


Figure 1. CCSD(T) optimized structures of minima and transition states on the potential energy surface of the $\text{CHCl}^{2+} + \text{H}_2$ reaction.

TABLE 1: CCSD(T)/cc-pVTZ Total Energies (ϵ_0), ZPE Corrections (ϵ_{ZPE}), and G2//CCSD(T)/cc-pVTZ Total Energies (E_0) for Optimized Stationary Point^a

ion	CCSD(T)/cc-pVTZ			G2//CCSD(T)/cc-pVTZ E_0 (hartree)
	total energy, ϵ_0 (hartree)	zero-point energy correction, ϵ_{ZPE} (hartree)	number of imaginary frequencies, N_{imag}	
HCCI ²⁺				
(M1)	-497.2561284	0.013103	0	-497.2624212
(M1*)	-497.1046050	0.010099	0	-497.1068969
HCCI ⁺ (M2)	-497.8949245	0.011787	0	-497.9013499
CCIH ²⁺				
(M3)	-497.1433105	0.008100	0	-497.1513534
(M3*)	-497.071144	0.009020	0	-497.0750002
CCIH ⁺ (M4)	-497.8039271	0.009000	0	-498.4060908
CCI ⁺				
(M5)	-497.2783858	0.002664	0	-497.2938751
(M5*)	-497.1615560	0.002505	0	-497.1731195
H ₂ CCI ⁺				
(M6)	-498.5824924	0.025311	0	-498.5784022
(M6*)	-498.4675510	0.021189	0	-498.4615406
CCIH ₂ ⁺ (M7)	-498.2858216	0.014765	0	-498.2963570
HCCIH ⁺				
<i>anti</i> -HCCIH ⁺ (<i>anti</i> -M8)	-498.4586091	0.020779	0	-498.4571974
<i>syn</i> -HCCIH ⁺ (<i>syn</i> -M8)	-498.4541564	0.020206	0	-498.4538246
(M8*)	-498.4430840	0.020018	0	-498.4377691
H ₂ HCCI ²⁺				
(M9)	-498.4704983	0.029096	0	-498.4623216
(M9*)	-499.0377061	0.027862	0	-498.4066984
H ₂ CCIH ²⁺				
(M10)	-498.5375510	0.033183	0	-498.5242254
(M10*)	-498.4003345	0.025417	0	-498.3905748
HCCI-H ₂ ²⁺ (M11)	-498.4378949	0.024936	0	-498.4367444
H ₂ -CCIH ²⁺				
<i>anti</i> -H ₂ -CCIH ²⁺ (<i>anti</i> -M12)	-498.3714302	0.022655	0	-498.3687874
<i>syn</i> -H ₂ -CCIH ²⁺ (<i>syn</i> -M12)	-498.3627802	0.022655	0	-498.3597843
TS1	-497.1096583	0.005105	1	-497.1217543
TS2	-498.4300125	0.023837	1	-498.4292027
TS3	-498.4450876	0.026906	1	-498.4381582
<i>anti</i> -TS4	-498.3622779	0.019380	1	-498.3578750
<i>syn</i> -TS4	-498.3569943	0.019581	1	-498.3497755
<i>anti</i> -TS5	-498.3733350	0.022866	1	-498.3694716
<i>syn</i> -TS5	-498.3637989	0.021975	1	-498.3613415
<i>anti</i> -TS6	-498.3698752	0.022592	1	-498.3666267
<i>syn</i> -TS6	-498.3646262	0.021608	1	-498.3636525
<i>anti</i> -TS6'	-498.3694698	0.020676	2	-498.3683203
<i>anti</i> -TS7	-498.3306316	0.019317	1	-498.3350259
<i>syn</i> -TS7	-498.3411639	0.019938	1	-498.3408807
TS8	-498.4507740	0.026015	1	-498.4471218
<i>anti</i> -TS9	-498.3572883	0.022264	1	-498.3555224
<i>syn</i> -TS9	-498.3565486	0.021758	1	-498.3552494
TS10	-498.4238672	0.015934	1	-498.4293405

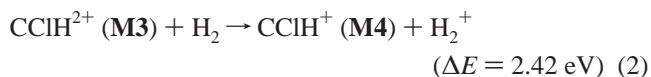
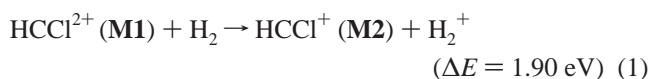
^a Values given in italics denote that the corresponding energy was calculated for the CCSD(T)/6-31++G** optimized structure.

(CCSD(T) gave a value of 1.96 eV). The ionization energies obtained from the AQCC calculations for HCCI⁺ and CCIH⁺ were 17.31 and 17.92 eV, respectively. The CCSD(T) ionization energies of the two isomeric cations were 17.38 and 17.98 eV, respectively.

To complement the information, we list here also the CCSD(T) calculated harmonic frequencies of both dication isomers. They are as follows: 2822.1 (σ_g), 1343.2 (σ_g), and 793.1(π) cm^{-1} for HCCI²⁺ and 2148.9 (a'), 752.4 (a'), and 654.1 (a') cm^{-1} for CCIH²⁺.

3.1. Charge Transfer: Formation of CHCl^+ . Charge transfer is usually the dominant process in reactions of dications with neutrals.¹⁻⁷ However, in the case of the reaction of CHCl^{2+} with D_2 (the same is true for H_2), the situation is different. According to the experimental results,¹⁰ the nondissociative charge-transfer reaction is only a minor process. The explanation seems to follow from the reaction window concept.²⁷ This concept predicts that charge transfer has a large cross section only if the reaction exoergicity is $\sim 2-5$ eV. Based on our

calculations, the exoergicities of the charge-transfer processes of the ground states of HCCI²⁺ and CCIH²⁺ with H_2 are only 1.90 and 2.42 eV, respectively.



The exoergicity ΔE is defined as a difference of G2 electronic energy of reactants and products, including the ZPE (see the E_0 values in Tables 1 and 2). Results of experimental studies of the CHCl^{2+} reaction with argon (which has an ionization energy, 15.75 eV, that is similar to that with H_2 , 15.43 eV) implied that both ground and excited states of CHCl^{2+} were involved in the charge-transfer process.¹¹ A comparison of the experimental data with the AQCC calculations¹² led to the conclusion that the states that contributed to the formation of

TABLE 2: Relative Energies (Related to the Total Energy of Reactants $\text{HCCl}^{2+} + \text{H}_2$) of Calculated Points on the Hypersurface of the Reaction $\text{HCCl}^{2+} + \text{H}_2^a$

	CCSD(T)/cc-pVTZ		G2
	$\Delta(\epsilon_0)_{\text{rel}}$	$\Delta(\epsilon + \epsilon_{\text{ZPE}})_{\text{rel}}$	$\Delta(E_0)_{\text{rel}}$
HCCl^{2+}			
(M1) + H_2	0	0	0
(M1*) + H_2	4.12	4.04	4.23
HCCl^+ (M2) + H_2^+	-1.87	-2.03	-1.90
CClH^{2+}			
(M3) + H_2	3.07	2.93	3.02
(M3*) + H_2	5.03	4.65	5.10
CClH^+ (M4) + H_2^+	0.61	0.37	0.60
CCl^+			
(M5) + H_3^+	-5.21	-5.21	-5.30
(M5*) + H_3^+	-2.03	-2.04	-2.02
(M5) + $\text{H}_2 + \text{H}^+$	-0.61	-0.89	-0.86
(M5*) + $\text{H}_2 + \text{H}^+$	2.57	2.29	2.43
H_2CCl^+			
(M6) + H^+	-4.19	-4.13	-4.09
(M6*) + H^+	-1.06	-1.12	-0.91
CClH_2^+ (M7) + H^+	3.88	3.65	3.59
HCClH^+			
<i>anti</i> - HCClH^+ (<i>anti</i> -M8) + H^+	-0.82	-0.88	-0.79
<i>syn</i> - HCClH^+ (<i>syn</i> -M8) + H^+	-0.70	-0.78	-0.70
(M8*) + H^+	-0.40	-0.48	-0.26
$\text{H}_2\text{HCCl}^{2+}$ (M9)	-1.14	-0.98	-0.93
$\text{H}_3\text{CCl}^{2+}$ (M9*)	-0.17	-0.04	0.17
$\text{H}_2\text{CClH}^{2+}$			
(M10)	-2.97	-2.70	-2.61
(M10*)	0.77	0.83	1.02
$\text{HCCl}-\text{H}_2^{2+}$ (M11)	-0.26	-0.21	-0.23
$\text{H}_2-\text{CClH}^{2+}$			
<i>anti</i> - $\text{H}_2-\text{CClH}^{2+}$ (<i>anti</i> -M12)	1.55	1.54	1.62
<i>syn</i> - $\text{H}_2-\text{CClH}^{2+}$ (<i>syn</i> -M12)	1.79	1.77	1.86
TS1 + H_2	3.99	3.77	3.83
TS2	-0.04	-0.02	-0.03
TS3	-0.45	-0.35	-0.27
<i>anti</i> -TS4	1.80	1.70	1.91
<i>syn</i> -TS4	1.94	1.85	2.13
<i>anti</i> -TS5	1.50	1.49	1.60
<i>syn</i> -TS5	1.76	1.73	1.82
<i>anti</i> -TS6	1.59	1.58	1.68
<i>syn</i> -TS6	1.74	1.70	1.76
<i>anti</i> -TS6'	1.61	1.54	1.63
<i>anti</i> -TS7	2.66	2.56	2.54
<i>syn</i> -TS7	2.38	2.29	2.38
TS8	-0.61	-0.53	-0.52
<i>anti</i> -TS9	1.94	1.91	1.98
<i>syn</i> -TS9	1.96	1.92	1.98
TS10	0.13	-0.07	-0.03

^a All values given in units of eV. Values given in italics denote that the corresponding energy was calculated for the CCSD(T)/6-31++G** optimized structure.

the charge-transfer products were the ground state of the isomer HCCl^{2+} (reaction), the ground state of the other isomer CClH^{2+} (reaction), and also the first excited triplet state of CClH^{2+} . This excited state is located 2.08 eV (AQCC calculation gave a value of 1.94 eV) above the ground state of CClH^{2+} , and, thus, the exoergicity of the charge-transfer process with H_2 is 4.50 eV, matching the reaction window very well.²⁷ Therefore, it was assumed that this state preferentially reacted via charge transfer and was not significantly involved in chemical reactions.

Figure 2a shows the relative translational-energy distribution $P(T')$ of the charge-transfer products $\text{CHCl}^+ + \text{D}_2^+$ plotted against the reaction exoergicity $\Delta E = T' - T$, as obtained from the experiments.¹⁰ Charge-transfer channels of the ground and the first electronic excited state of the isomer CClH^{2+} (exoergicities marked with solid arrows in Figure 2a) explain the bulk of the broad peak of the $P(T')$ curve. The ground state of the dication reactant HCCl^{2+} contributes to the charge-transfer

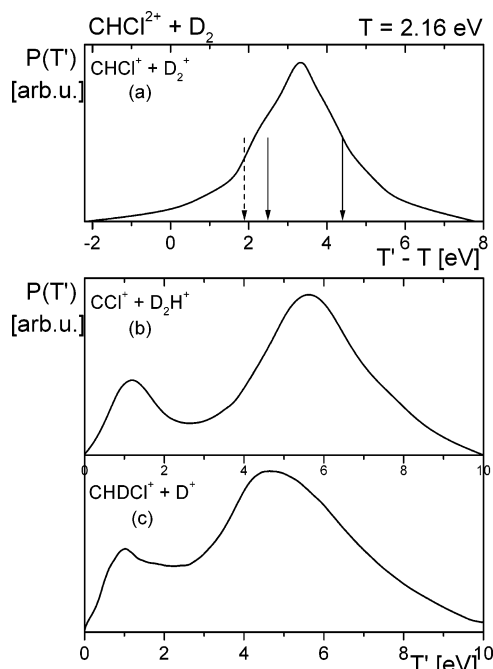
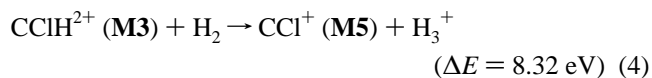
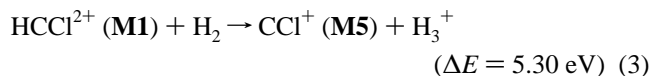


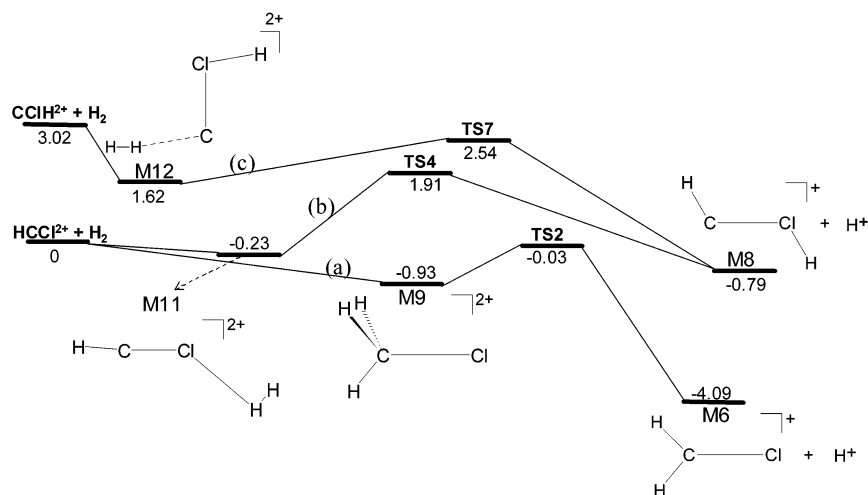
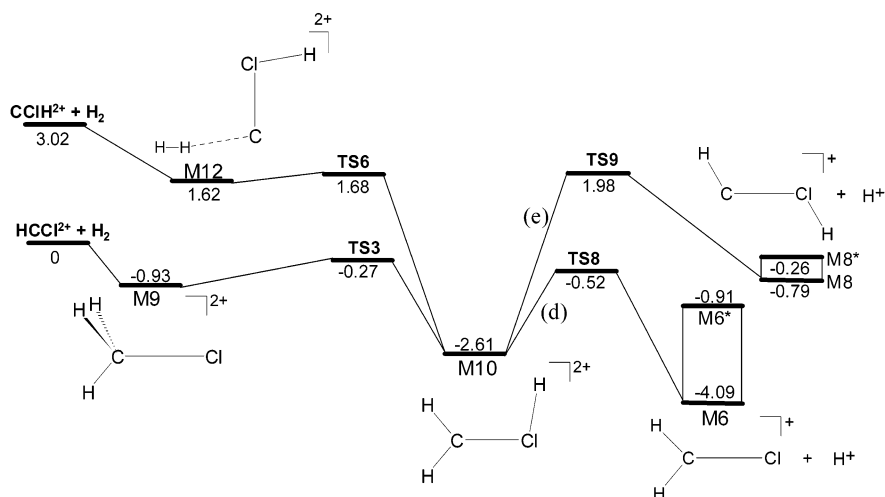
Figure 2. Relative translational-energy distributions, $P(T')$, of products (a) $\text{CHCl}^+ + \text{D}_2^+$, (b) $\text{CCl}^+ + \text{D}_2\text{H}^+$, and (c) $\text{CHDCl}^+ + \text{D}^+$ from collisions of $\text{CHCl}^{2+} + \text{D}_2$ ($T = 2.16 \text{ eV}$) plotted against the reaction exoergicity $\Delta E = T' - T$ (panel a) or product-relative translational energy T' (panels b and c).

channels only marginally (dashed arrow in Figure 2a). For a more detailed discussion of the charge-transfer results and the role of excited states of CHCl^{2+} in this reaction, see the companion paper in this issue.¹⁰

3.2. Formation of CCl^+ (M5). The major process in the reaction of CHCl^{2+} with D_2 (the same holds for H_2) is the formation of CCl^+ . The product ion CCl^+ originates mainly in proton transfer from the dication CHCl^{2+} to molecular H_2 , which is characterized by a rather high exoergicity. Both isomers of the dication can react:

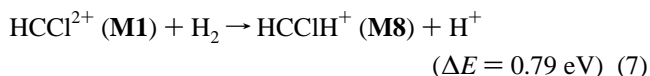
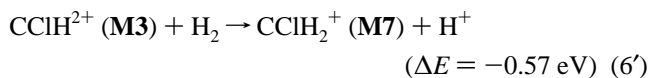
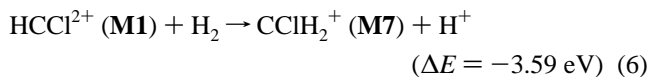
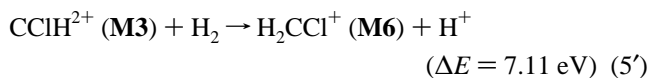
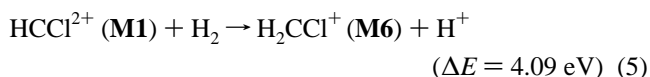


All attempts to localize a transition state for the proton transfer from either HCCl^{2+} or CClH^{2+} to the molecule H_2 were unsuccessful. The optimization of the corresponding structures led to a stationary point of a higher order or led to dissociation into CCl^+ and H_3^+ . This finding, which implies no intermediate in this reaction, is in agreement with the conclusion from the experimental results,¹⁰ namely that the proton-transfer reaction is a direct process, which is characterized by a strong forward scattering of the product CCl^+ . The relative translational-energy distribution of the products $\text{CCl}^+ + \text{HD}_2^+$, $P(T')$ vs T' , is shown in Figure 2b. The proton transfer to D_2 causes the broad peak that is located in the range of 3–10 eV in the $P(T')$ curve (the collision energy T was 2.16 eV). The smaller peak, at ~1.2 eV, results from a further decomposition of the charge-transfer product CHDCl^+ and will be discussed in Section 3.4. The calculated exoergicities suggest that the dication reactant in the proton-transfer reaction is mainly the ground state of the isomer HCCl^{2+} (M1; see reaction 3), with a less significant contribution from CClH^{2+} (M3, see reaction 4).

SCHEME 1. Pathways to $[\text{CH}_2\text{Cl}^+]$ via "Loosely Bound" ComplexesSCHEME 2. Pathways to $[\text{CH}_2\text{Cl}^+]$ via "Stable" Intermediate M10

The triplet excited state of CCl^+ (M5^*) lies 3.29 eV above the ground state M5 (the AQCC excitation energy is 3.16 eV).

3.3. Formation of H_2CCl^+ (M6) and HCClH^+ (M8) in Chemical Reactions. The calculated exoergicities of the possible processes between reactant dication isomers and product ion isomers are as follows:



Three stable isomers are considered for the product of the

chemical reaction between the dications HCCl^{2+} (M1) and CClH^{2+} (M3) (see Figure 1a). The isomer H_2CCl^+ (M6) has both H atoms attached to the C atom, CClH_2^+ (M7) has both H atoms bonded to the Cl atom, and finally HCClH^+ (M8) has one H atom attached to the C atom and the other one to the Cl atom. In addition, this $\text{H}-\text{C}-\text{Cl}-\text{H}^+$ isomer can exist in two rotamers: either as *anti*- M8 , with the anti-periplanar arrangement of the H atoms (torsion angle of 180°), or as *syn*- M8 , with syn-periplanar arrangement of the two H atoms (torsion angle of 0°). A rotational barrier of a considerable height (0.64 eV) was observed for the transition from *anti*- M8 to *syn*- M8 . The anti-periplanar arrangement is more stable than the syn-periplanar arrangement, by 0.09 eV.

All energies given in Schemes 1 and 2 refer to the more-stable anti-isomers. Energies of the corresponding syn-structures can be found in Tables 1 and 2 and in the following text. In addition to the singlet states, triplet states of H_2CCl^+ and HCClH^+ were also optimized. They are denoted by an asterisk (*) in Tables 1 and 2 and in Figure 1a. Optimization of the structure of the cation CClH_2^+ in the triplet state led to its dissociation along the C-Cl bond.

The calculated reaction pathways have a common feature. The first step is the formation of a "loosely bound" complex between the original dication and H_2 , with the charge being delocalized over the entire complex. In the second step, this complex either dissociates directly to $[\text{CH}_2\text{Cl}]^+ + \text{H}^+$ or

rearranges to the dication $\text{H}_2\text{CCH}^{2+}$. The pathways following the direct dissociation are summarized in Scheme 1, whereas the pathways that lead to other dissociations via rearrangement are summarized in Scheme 2.

3.3.1. "Loosely Bound" Intermediates. First, the formation of the loosely bound complexes will be discussed. The H_2 molecule can attack the dication HCCl^{2+} at two sites, either at the C atom or at the Cl atom. Attack at the carbon site leads to the intermediate $\text{H}_2\text{HCCl}^{2+}$ (**M9**). The two newly formed C–H bonds are longer (1.34 Å) than the original C–H bond (1.10 Å). This dication was described earlier by Duflo et al.,⁶ and the corresponding CASSCF calculated geometry is given in parentheses in Figure 1a. The $\text{H}_3\text{CCl}^{2+}$ structure with three equivalent C–H bonds exists as a stationary point in its triplet state (**M9***); the excitation energy is 1.10 eV. The intermediate $\text{H}_2\text{HCCl}^{2+}$ (**M9**) can eliminate directly one proton via the transition state (**TS2**, Scheme 1): through the asymptotic mode, one of the distant H atoms gets closer to the C atom, whereas the other H atom is removed as a proton. The barrier height of this process is 0.90 eV. The barrier height of the competing process, which is the rearrangement to the $\text{H}_2\text{CCH}^{2+}$ intermediate (**M10**) through the transition state **TS3** (Scheme 2), is only 0.66 eV. This barrier is 0.24 eV (~30%) lower than the barrier for direct dissociation; therefore, the rearrangement via **TS3** may be expected to proceed more efficiently.

An attack of H_2 at the Cl site of HCCl^{2+} (**M1**) results in the formation of the intermediate $\text{HCCl}-\text{H}_2^{2+}$ (**M11**). The distances of both H atoms to the Cl atom are rather large: 2.49 and 2.55 Å, respectively. Not surprisingly, the H_2 molecule bound to the Cl atom is only slightly perturbed; the length of the H–H bond is 0.76 Å, which is quite close to the equilibrium distance of an isolated molecule H_2 . The intermediate **M11** loses one proton via the transition state **TS4**. The barrier height for the formation of the anti-isomer via *anti-TS4* is 2.14 eV, and the barrier height for the formation of the syn-isomer via *syn-TS4* is 2.36 eV. The removal of the H atom that is bonded to the C atom, and the subsequent formation of CCH_2^+ (**M7**), can be neglected. This reaction is very endoergic (3.59 eV); thus, it was not accessible under the conditions of the performed experiments (the collision energy was ≤ 2.16 eV).

The other isomer of the reactant dication, CCH^{2+} (**M3**), also can be attacked at two sites. An attack of the H_2 molecule at the C site results in the formation of the intermediate $\text{H}_2-\text{CCH}^{2+}$ (**M12**), where the incoming H_2 molecule is bound via one H atom to a C atom. Again, two rotamers (anti- and syn-) were found and the following analysis is given only for the anti-isomer. The surface of the syn-isomer shows analogous features and the corresponding values can be found in Tables 1 and 2. The structure **M12** was found as a true minimum with all frequencies being real at the CCSD(T)/6-31++G** level. Increasing the basis set to cc-pVTZ led to a rearrangement to the ylide dication $\text{H}_2\text{CCH}^{2+}$ (**M10**). A quick check of the size of the basis set dependence for the intermediate **M12** was made on the B3LYP level with basis sets 6-31G**, 6-31++G**, 6-311G**, 6-311++G(3dp,3df), cc-pVDZ, cc-pVTZ, and aug-cc-pVTZ, as implemented in Gaussian 98. A minimum for the intermediate **M12** was found only with the smallest 6-31G** and 6-31++G** basis sets. When increasing the basis set to a triple- ζ quality, the structure **M12** could not be located as a stationary point. All calculations resulted in the structure $\text{H}_2\text{CCH}^{2+}$ (**M10**). Nevertheless, a transition state, which represents the barrier for the "out-of-plane" rotation of the H_2 molecule bound to the C atom (**TS5**), could be identified, using the CCSD(T)/cc-pVTZ method. The length of the H–H bond

was, in this case, 0.84 Å and the distance from the center of the H–H bond to the C atom was 1.51 Å. The energy values in Tables 1 and 2, and Schemes 1 and 2 for **M12** correspond to the CCSD(T)/cc-pVTZ single-point energy calculation for the CCSD(T)/6-31++G** optimized structure. The ZPE was also derived from the CCSD(T)/6-31++G** calculations. The rotational barrier (**TS5**) has a slightly lower energy (by 0.02 eV) than the energy obtained in this way for **M12**. Therefore, the existence of **M12** seems to be highly questionable. This implies that the intermediate **M12** is, very likely, a shoulder on the relevant PES, rather than a distinct minimum, and that it rearranges to the intermediate $\text{H}_2\text{CCH}^{2+}$ (**M10**). Consequently, the optimization the corresponding transition state (**TS6**) for this rearrangement is associated with similar difficulties. A transition state with a single imaginary frequency exists only at the CCSD(T)/6-31++G** level. The correct identification of the reaction path was checked by calculating the intrinsic reaction coordinate (IRC)²⁸ at the B3LYP/6-31++G** level. The barrier height is rather small (0.06 eV). When using the triple- ζ basis set (cc-pVTZ), either with the CCSD(T) or the B3LYP method, only a second-order transition state (**TS6'**) could be located in this area of the PES. The two imaginary frequencies were characterized as follows: one represents the desired mode (i.e., the same imaginary frequency as that observed for **TS6**), and the second represents an "out-of-plane" rotation of the H_2 fragment that is bonded to the C atom. The IRC calculations at the B3LYP/cc-pVTZ level lead to $\text{H}_2\text{CCH}^{2+}$ (**M10**) in one direction and to the **TS5** in the other direction. The calculated barrier height was 0.01 eV. Finally, it could be concluded that **M12**, if existing at all, was only a very flat minimum, with a depth presumably below the ZPE.

The direct breakup of the intermediate $[\text{H}_2-\text{CCH}]^{2+}$ (**M12**) to the products HCCl^+ (**M8**) + H^+ proceeds via the transition state **TS7**, identified as a real transition state also at the CCSD(T)/cc-pVTZ level with a single imaginary frequency of $i1118.5\text{ cm}^{-1}$ (*anti-TS7*) and $i927.7\text{ cm}^{-1}$ (*syn-TS7*), characterizing the proper PES curvature. The barrier height calculated for the formation of *anti-M8* (with *anti-TS7*) was 0.92 eV, and that which was calculated for the formation of *syn-M8* (with *syn-TS7*) was 0.52 eV.

The isomer CCH_2^+ (**M7**), which is lying at a rather high energy, should be formed by an attack of the H_2 molecule at the Cl end of the CCH^{2+} reactant. However, all attempts to optimize its structure with the proper connectivity, i.e., with all three H atoms bound to the Cl atom, led to dissociation of the C–Cl bond.

3.3.2. Dissociation of the Dication $\text{H}_2\text{CCH}^{2+}$ (M10**).** The intermediate $\text{H}_2\text{CCH}^{2+}$ (**M9**) can lose a proton either from the C atom or from the Cl atom. Breaking the Cl–H bond is less demanding, from an energy standpoint. In addition to the proton, the product ion H_2CCl^+ (**M6**) is formed in this dissociation process. The respective transition state **TS8** is connected with a barrier height of 2.09 eV.

The process, which requires more energy and the breaking of the C–H bond, leads to the product pair $\text{HCCl}^+ + \text{H}^+$. Again, the breaking of the C–H bond may occur in the syn-periplanar or anti-periplanar position, with respect to the C–Cl bond. Breaking the syn-periplanar C–H bond (*anti-TS9*) leads to the anti-isomer (*anti-M8*), and the barrier height is 4.59 eV. The optimized transition-state structures have rather long C–H bonds: 3.26 Å in the *anti-TS9* and 3.27 Å in the *syn-TS9* (Figure 1). Thus, the barrier height for breaking the anti-periplanar C–H bond is as large as the barrier height for breaking the syn-periplanar C–H bond (4.59 eV).

3.3.3. *Application to Experimental Data.* Theoretical information on the reactants, intermediates, transition states, and products, as well as on the calculated reaction pathways, was then applied to the available experimental data on the reaction $\text{CHCl}^{2+} + \text{D}_2$.^{4,10} The ion product CD_2Cl^+ could not be identified among the reaction products (its intensity was beyond the limit of detection, i.e., <20% of the intensity of the product CHDCI^+).¹⁰ Therefore, the pathways that lead either to this product or to a mixture of CHDCI^+ and CD_2Cl^+ were excluded from these considerations. The relative translational-energy distribution of the products $\text{CHDCI}^+ + \text{D}^+$ is characterized by two peaks in the $P(T')$ vs T' dependence (see Figure 2c). The major peak lies at ~ 4.7 eV. The analysis of the scattering results indicated that the products connected with this translational-energy release were formed by a decomposition of a short-lived intermediate of a mean lifetime of $\sim 10^{-12}$ s. The second process is characterized by a translational-energy release of ~ 1.1 eV, and the relevant portion of the scattering suggested that the product was formed via a decomposition of a long-lived complex intermediate of a mean lifetime that is considerably longer than $\sim 10^{-12}$ s.

The measured translational-energy release of processes that are associated with the decomposition of the intermediates can be related to the exit barrier heights on the way from the transition state to the products. All pathways shown in Scheme 1 (a, b, c), i.e., direct dissociation of "loosely bound" intermediates, lead to CHDCI^+ . The common step in these processes is the formation of the complex $[\text{D}_2\text{-CHCl}]^{2+}$; in the next step, one D atom is bonded to the C or Cl atom and the other leaves as D^+ . "Loosely bound" intermediates represent short-lived complexes. The exit barrier heights for pathways a and c are 4.06 and 3.33 eV, respectively. After including the collision energy (2.16 eV), the resulting values match the upper portion of the $P(T')$ curve in Figure 2c reasonably well, in the range from ~ 3.5 eV to 8 eV, with a maximum at ~ 5 eV.

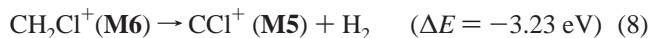
The pathways that lead through the intermediate $\text{H}_2\text{CCH}^{2+}$ (**M10**) had to be analyzed individually. The reaction of HCCl^{2+} with D_2 will primarily result in the formation of the complex $\text{D}_2\text{-CHCl}^{2+}$ (**M9**), which rearranges to DHCClD^{2+} (**M10**), with one D atom being bound to the C atom and the other being bound to the Cl atom. This mechanism was confirmed by an IRC calculation from the transition state **TS3** at the B3LYP/cc-VTZ level. This intermediate will lose D^+ from the Cl atom more efficiently via the transition state **TS8** (pathway d), because the activation barrier is 2.50 eV, which is >50% lower than the activation barrier for dissociation via **TS9** (see pathway e). The transition state **TS9** is associated with the hydrogen loss from the C atom; thus, it would lead to a mixture of two products: HDCCl^+ and D_2CCl^+ . This is, however, in conflict with the experimental observation.

The reaction of the other isomer, CClH^{2+} , with deuterium leads eventually to the complex $[\text{D}_2\text{-CClH}]^{2+}$ (**M12**), which, in the next step, rearranges to $\text{D}_2\text{CClH}^{2+}$ (**M10**), with both D atoms being bonded to the C atom. Dissociation via the lower transition state **TS8** (pathway d) leads to a loss of the proton from the Cl atom and to the formation of the product D_2CCl^+ . To explain why this product is not experimentally observed, one must realize that, at the collision energy of 2.16 eV, the total excess energy—with respect to the minimum **M10**—is 7.79 eV. If the D_2CCl^+ were formed via pathway d, it would possess a very large internal energy that would very likely lead to its dissociation (see Section 3.4). The pathway that leads through the transition state **TS9** (pathway e) with a much higher barrier

leads to the product DCClH^+ . However, because of the high barrier height, this process is less likely.

The ylide intermediate represents a long-lived complex; however, the exit barrier height for pathway d, 3.58 eV (3.69 eV, including the ZPE), is larger than the experimentally observed energy release (1.1 eV). However, the ylide intermediate possesses a rather high internal excitation; thus, it seems that this process may lead to the formation of an electronic excited state of the product DHCCl^+ . An excited state of H_2CCl^+ was calculated to lie 3.18 eV above the ground state, and this value would fit the experimental results reasonably well.

3.4. **Further Decomposition of CH_2Cl^+ .** The cation CH_2Cl^+ can decompose via a loss of a H_2 molecule:



This endoergic process proceeds via the transition state **TS10**, and the barrier height is 4.06 eV.

From the theoretical analysis and a comparison with the experimental data,¹⁰ it was concluded that the low-energy peak in the relative translational-energy distribution of CCl^+ (see Figure 1b) originates from further decomposition of a vibrationally excited product CHDCI^+ . As mentioned previously, the cation CD_2Cl^+ , which is formed in the reaction of CClH^{2+} with D_2 via the decomposition of the intermediate $\text{D}_2\text{CClH}^{2+}$, should possess a large internal excitation; thus, it could easily decompose to CCl^+ and D_2 . However, this cannot be proven experimentally, because the product CD_2Cl^+ could not be observed in measurable amounts.

4. Heats of Formation

The present study makes it possible to estimate the heats of formation, $\Delta_f H$, of the species $\text{CH}_x\text{Cl}^{n+}$ (where $x = 0, 1, 2$ and $n = 1, 2$) involved. For the cations, related published experimental data can be used in the derivation. For the dications, the estimation was based on enthalpies of reactions as described in this paper. The data and reactions used are summarized in Table 3.

The heat of formation of the cation HCCl^+ , $\Delta_f H^\circ(\text{HCCl}^+) = 1284$ kJ/mol, was determined from the published data for the carbene HCCl ($\Delta_f H^\circ(\text{HCCl}) = 334.7$ kJ/mol,²⁹ $\text{IE}(\text{HCCl}) = 9.84$ eV³⁰). In a similar way, the heat of formation of CCl^+ , $\Delta_f H^\circ(\text{CCl}^+) = 1360$ kJ/mol, was obtained from $\Delta_f H^\circ(\text{CCl}) = 502$ kJ/mol²⁹ and $\text{IE}(\text{CCl}) = 8.9 \pm 0.2$ eV.³¹ For H_2CCl^+ , the heat of formation was determined as a sum of $\Delta_f H^\circ(\text{H}_2\text{CCl}^-)$ (66.3 kJ/mol³²), $\text{IE}(\text{H}_2\text{CCl})$ (8.75 ± 0.01 eV³³), and the electron affinity of H_2CCl (0.74 ± 0.16 eV³⁴); $\Delta_f H^\circ(\text{H}_2\text{CCl}^+) = 982$ kJ/mol.

The estimation of heats of formation of ions in Table 3 was based on reactions in which these ions are produced from cations of known $\Delta_f H^\circ$, as obtained previously (CCl^+ , HCCl^+ , and H_2CCl^+), and tabulated data for $\Delta_f H^\circ(\text{H}) = 218$ kJ/mol, and $\Delta_f H^\circ(\text{H}^+) = 1530$ kJ/mol.³⁵ For calculation of the reaction enthalpies ($\Delta_r H$), the values of $E_0(\text{G2})$ energies and $\epsilon_0(\text{CCSD(T)})$ were used as given in Table 1. The values of $\Delta_r H$ corrected for ZPE ($\epsilon_0 + \epsilon_{\text{ZPE}}$) and the values that had been corrected for internal thermal energy (E_{tr} , E_{rot} , E_{vib} , E_e) and the factor $k_b T$, implemented in the Gaussian 98 as a thermal correction to the enthalpy H_{corr} ,¹⁸ also were tested. The tests were conducted for calculations of the $\Delta_f H^\circ$ values of CCl^+ , HCCl^+ , and H_2CCl^+ (see the upper portion of Table 3). The values of $\Delta_r H$ that were calculated from ϵ_0 led to the best agreement with the experimental data and the smallest error of the mean. Using the $E_0(\text{G2})$ energies (Table 1), the heat of formation of the dication

TABLE 3: Estimation of Heats of Formation ($\Delta_f H^\circ$)^a of the Dications HCCl^{2+} and CClH^{2+} and the Cations CClH^+ and HCClH^+

ion	equation	$\Delta_f H$ calculated from tabulated data (kJ/mol)			
CCl^+	$\Delta_f H(\text{CCl}) + \text{IE}(\text{CCl})$	1360.80 ± 19.30			
HCCl^+	$\Delta_f H(\text{HCCl}) + \text{IE}(\text{HCCl})$	1284.14			
H_2CCl^+	$\Delta_f H(\text{H}_2\text{CCl}^+) + \text{EA}(\text{H}_2\text{CCl}) + \text{IE}(\text{H}_2\text{CCl})$	981.97			
		CCSD(T)		G2	
ion	reaction	estimated $\Delta_f H$ (kJ/mol)	average \pm SEM ^b	estimated $\Delta_f H$ (kJ/mol)	average \pm SEM ^b
CCl^+	$\text{H}_2\text{CCl}^+ \rightarrow \text{CCl}^+ + \text{H}_2$	1327.9		1293.8	
	$\text{HCCl}^+ \rightarrow \text{CCl}^+ + \text{H}$	1372.6	1350.3 ± 18.2	1348.3	1321.0 ± 22.3
HCCl^+	$\text{H}_2\text{CCl}^+ \rightarrow \text{HCCl}^+ + \text{H}$	1256.9		1228.8	
	$\text{H} + \text{CCl}^+ \rightarrow \text{HCCl}^+$	1272.3	1264.6 ± 6.3	1296.6	1262.7 ± 27.7
H_2CCl^+	$\text{HCCl}^+ + \text{H} \rightarrow \text{H}_2\text{CCl}^+$	1009.2		1037.3	
	$\text{CCl}^+ + \text{H}_2 \rightarrow \text{H}_2\text{CCl}^+$	1014.8	1012.0 ± 2.3	1049.0	1043.2 ± 4.8
HCCl^{2+}	$\text{HCCl}^+ \rightarrow \text{HCCl}^{2+}$	2961.3		2961.6	
	$\text{H}_2\text{CCl}^+ \rightarrow \text{HCCl}^{2+} + \text{H}^-$	3016.1	2975.5 ± 20.6	2982.2	2972.4 ± 6.0
	$\text{H}^+ + \text{CCl}^+ \rightarrow \text{HCCl}^{2+}$	2949.2		2973.4	
CClH^{2+}	$\text{CClH}^+ \rightarrow \text{CClH}^{2+}$	3257.5		3253.3	
	$\text{H}^+ + \text{CCl}^+ \rightarrow \text{CClH}^{2+}$	3245.4	3271.7 ± 20.6	3265.0	3264.0 ± 6.0
	$\text{H}_2\text{CCl}^+ \rightarrow \text{CClH}^{2+} + \text{H}^-$	3312.3		3273.8	
CClH^+	$\text{HCCl}^+ \rightarrow \text{CClH}^+$	1523.1		1525.6	
	$\text{H} + \text{CCl}^+ \rightarrow \text{CClH}^+$	1511.2	1510.1 ± 7.9	1538.1	1511.4 ± 20.8
	$\text{H}_2\text{CCl}^+ \rightarrow \text{CClH}^+ + \text{H}$	1495.8		1470.3	
HCClH^+	$\text{HCCl}^+ + \text{H} \rightarrow \text{HCClH}^+$	1334.4		1355.5	
	$\text{CCl}^+ + \text{H}_2 \rightarrow \text{HCClH}^+$	1340.1	1327.3 ± 10.2	1367.2	1341.0 ± 20.7
	$\text{H}_2\text{CCl}^+ \rightarrow \text{HCClH}^+$	1307.2		1300.2	

^a $\Delta_f H$ values for CCl^+ , HCCl^+ , and H_2CCl^+ were calculated from tabulated data.^{29–34} ^b SEM = standard error of the mean.

HCCl^{2+} is $\Delta_f H^\circ(\text{HCCl}^{2+}) = 2972 \pm 6.0$ kJ/mol, and the heat of formation of the isomer dication CClH^{2+} is $\Delta_f H^\circ(\text{CClH}^{2+}) = 3264 \pm 6.0$ kJ/mol. The calculations give $\Delta_f H^\circ(\text{CClH}^+) = 1511 \pm 20$ kJ/mol, for the heat of formation of the isomer cation CClH^+ , and finally $\Delta_f H^\circ(\text{HCClH}^+) = 1341 \pm 21$ kJ/mol (which is the value for the anti-isomer).

5. Conclusions

(1) The potential energy surface of the $\text{CHCl}^{2+} + \text{D}_2$ system was investigated using the CCSD(T)/cc-pVTZ method, to determine the reaction pathways that lead to the experimentally observed products CHCl^+ , CHDCl^+ , and CCl^+ .

(2) The product CHCl^+ was determined to be the product of a nondissociative charge-transfer process between the two isomers of CHCl^{2+} (HCCl^{2+} and CClH^{2+}) and D_2 . The main contribution comes from the ground and first excited state of CClH^{2+} , giving the ground state of $\text{CClH}^+ + \text{D}_2^+$ (with calculated exoergicities of 2.42 and 4.50 eV, respectively). The contribution of charge transfer with the ground state of HCCl^{2+} (with an exoergicity of 1.90 eV) is minor.

(3) The product CCl^+ results mainly from a proton-transfer reaction between the ground state of HCCl^{2+} and D_2 and leads to CCl^+ and D_2H^+ (exoergicity of 5.30 eV). The proton-transfer reaction with the ground state of CClH^{2+} (exoergicity of 8.32 eV) also may contribute to the formation of the products. The calculated reaction pathways are in agreement with the experimental data.

(4) In the chemical reaction of CHCl^{2+} with H_2 , which leads to the products $[\text{CH}_2\text{Cl}]^+ + \text{H}^+$, the formation of two isomers of the molecular product— H_2CCl^+ and HCClH^+ —was investigated. With the reactant dication HCCl^{2+} , the formation of H_2CCl^+ is associated with an exoergicity of 4.09 eV, and the formation of HCClH^+ is associated with an exoergicity of 0.79 eV. With the reactant dication CClH^{2+} , the respective exoergicities are 7.11 eV for the formation of H_2CCl^+ , and 3.81

eV for the formation of HCClH^+ . In general, two types of pathways lead to the product formation. One leads directly to the reaction products through a loosely bound complex ($[\text{H}_2-\text{CHCl}]^{2+}$). The other one involves the formation of a “stable” intermediate $\text{H}_2\text{CClH}^{2+}$, which can dissociate to the products either by losing a proton from the Cl atom or by losing a proton from the C atom (a less likely case).

(5) A dissociation pathway for the formation of $\text{H}_2\text{CCl}^+ + \text{H}^+$ also was observed. This pathway was associated with a process that was endoergic by 3.23 eV.

(6) Using the calculated data and published thermodynamic information on several cations, the heats of formation of the dication isomers HCCl^{2+} and CClH^{2+} , and those of the cations CClH^+ and HCClH^+ , were estimated.

Acknowledgment. Partial support of this research by Grant No. 203/00/0632 from the Grant Agency of the Czech Republic and by Grant No. IAB4040302 of the Grant Agency of the Academy of Sciences is gratefully acknowledged. The work is also a part of the European Network MCI (Generation, Structure and Reaction Dynamics of Multiply-Charged Ions).

References and Notes

- Price, S. D.; Manning, M.; Leone, S. R. *J. Am. Chem. Soc.* **1994**, *116*, 8673.
- Dolejšek, Z.; Fárník, M.; Herman, Z. *Chem. Phys. Lett.* **1995**, *235*, 99.
- Herman, Z.; Žabka, J.; Dolejšek, Z.; Fárník, M. *Int. J. Mass Spectrom.* **1999**, *192*, 191.
- Newson, K. A.; Price, S. D. *Chem. Phys. Lett.* **1998**, *294*, 223.
- Newson, K. A.; Price, S. D. *Chem. Phys. Lett.* **1997**, *269*, 93.
- Mrázek, L.; Žabka, J.; Dolejšek, Z.; Hrušák, J.; Herman, Z. *J. Phys. Chem. A* **2000**, *104*, 7294.
- Tafadar, N.; Kearney, D.; Price, S. D. *J. Chem. Phys.* **2001**, *115*, 8819.
- Tafadar, N.; Price, S. D. *Int. J. Mass Spectrom.* **2003**, *223*, 547.
- Olah, G. A. *J. Org. Chem.* **2001**, *66*, 5943.

- (10) Roithová, J.; Žabka, J.; Hrušák, J.; Thissen, R.; Herman, Z. *J. Phys. Chem. A* **2003**, *107*, 7347.
- (11) Roithová, J.; Žabka, J.; Thissen, R.; Herman, Z. *J. Phys. Chem. Chem. Phys.* **2003**, *5*, 2988.
- (12) Roithová, J.; Hrušák, J.; Herman, Z. *Int. J. Mass Spectrom.* **2003**, *228*, 497.
- (13) Roithová, J.; Thissen, R.; Žabka, J.; Franceschi, P.; Dutuit, O.; Herman, Z. *Int. J. Mass Spectrom.* **2003**, *228*, 487.
- (14) Thissen, R.; Simon, M.; Hubin-Franskin, M. *J. Chem. Phys.* **1994**, *101*, 7548.
- (15) Dufлот, D.; Robbe, J.-M.; Flament, J.-P. *Int. J. Mass Spectrom. Ion Processes* **1997**, *171*, 215.
- (16) Yates, B. F.; Bouma, W. J.; Radom, L. *J. Am. Chem. Soc.* **1986**, *108*, 6545.
- (17) Dufлот, D.; Robbe, J.-M.; Flament, J.-P. *J. Chem. Phys.* **1995**, *103*, 10571.
- (18) Cížek, J. *Adv. Chem. Phys.* **1969**, *14*, 35.
- (19) Purvis, G. D.; Bartlett, R. J. *J. Chem. Phys.* **1982**, *76*, 1910.
- (20) Scuseria, G. E.; Janssen, C. L.; Schaefer, H. F., III. *J. Chem. Phys.* **1988**, *89*, 7382.
- (21) Scuseria, G. E.; Schaefer, H. F., III. *J. Chem. Phys.* **1989**, *90*, 3700.
- (22) Dunning, T. H., Jr. *J. Chem. Phys.* **1989**, *90*, 1007.
- (23) Kendall, R. A.; Dunning, T. H., Jr.; Harrison, R. J. *J. Chem. Phys.* **1992**, *96*, 6796.
- (24) Woon, D. E.; Dunning, T. H., Jr. *J. Chem. Phys.* **1993**, *98*, 1358.
- (25) Frisch, M. J.; Trucks, G. W.; Schlegel, H. B.; Scuseria, G. E.; Robb, M. A.; Cheeseman, J. R.; Zakrzewski, V. G.; Montgomery, J. A., Jr.; Stratmann, R. E.; Burant, J. C.; Dapprich, S.; Millam, J. M.; Daniels, A. D.; Kudin, K. N.; Strain, M. C.; Farkas, O.; Tomasi, J.; Barone, V.; Cossi, M.; Cammi, R.; Mennucci, B.; Pomelli, C.; Adamo, C.; Clifford, S.; Ochterski, J.; Petersson, G. A.; Ayala, P. Y.; Cui, Q.; Morokuma, K.; Malick, D. K.; Rabuck, A. D.; Raghavachari, K.; Foresman, J. B.; Cioslowski, J.; Ortiz, J. V.; Stefanov, B. B.; Liu, G.; Liashenko, A.; Piskorz, P.; Komaromi, I.; Gomperts, R.; Martin, R. L.; Fox, D. J.; Keith, T.; Al-Laham, M. A.; Peng, C. Y.; Nanayakkara, A.; Gonzalez, C.; Challacombe, M.; Gill, P. M. W.; Johnson, B. G.; Chen, W.; Wong, M. W.; Andres, J. L.; Head-Gordon, M.; Replogle, E. S.; Pople, J. A. *Gaussian 98*, revision A.11; Gaussian, Inc.: Pittsburgh, PA, 1998.
- (26) Curtiss, L. A.; Raghavachari, K.; Trucks, G. W.; Pople, J. A. *J. Chem. Phys.* **1991**, *94*, 7221.
- (27) Olson, R. E. *J. Chem. Phys.* **1972**, *56*, 2976.
- (28) Gonzalez, C.; Schlegel, H. B. *J. Chem. Phys.* **1989**, *90*, 2154.
- (29) Chase, M. W., Jr. *J. Phys. Chem. Ref. Data, Monogr.* **1998**, *9*, 1–1951.
- (30) Lias, S. G.; Karpas, Z.; Liebman, J. F. *J. Am. Chem. Soc.* **1985**, *107*, 6089.
- (31) Hepburn, J. W.; Trevor, D. J.; Pollard, J. E.; Shirley, D. A.; Lee, Y. T. *J. Chem. Phys.* **1982**, *76*, 4287.
- (32) Poutsma, J. C.; Nash, J. J.; Paulino, J. A.; Squires, R. R. *J. Am. Chem. Soc.* **1997**, *119*, 4687.
- (33) Andrews, L.; Dyke, J. M.; Jonathan, N.; Keddar, N.; Marris, A. *J. Am. Chem. Soc.* **1997**, *119*, 44686.
- (34) Ingemann, S.; Nibbering, N. M. M. *J. Chem. Soc., Perkin Trans.* **1985**, 837.
- (35) Lias, S. G.; Bartmess, J. E.; Liebmann, J. F.; Holmes, J. L.; Levin, R. D.; Mallard, W. C. *J. Phys. Chem. Ref. Data, Suppl.* **1988**, *17*, (1).